Contract No:

This document was prepared in conjunction with work accomplished under Contract No. DE-AC09-08SR22470 with the U.S. Department of Energy (DOE) Office of Environmental Management (EM).

Disclaimer:

We put science to work.™

Savannah River National Laboratory™

OPERATED BY SAVANNAH RIVER NUCLEAR SOLUTIONS

A U.S. DEPARTMENT OF ENERGY NATIONAL LABORATORY • SAVANNAH RIVER SITE • AIKEN, SC

Velocity Field Calculation For Non-Orthogonal Numerical Grids

G. P. Flach

March 2015

SRNL-STI-2015-00115, Revision 0

DISCLAIMER

Printed in the United States of America

Prepared for
U.S. Department of Energy

SRNL-STI-2015-00115
Revision 0

Keywords: *Porous-medium flow*
Performance Assessment
Groundwater modeling
PORFLOW

Retention: *Permanent*

Velocity Field Calculation For Non-Orthogonal Numerical Grids

G. P. Flach

March 2015

Prepared for the U.S. Department of Energy under contract number DE-AC09-08SR22470.

Savannah River National Laboratory ™

OPERATED BY SAVANNAH RIVER NUCLEAR SOLUTIONS

REVIEWS AND APPROVALS

AUTHORS:

G. P. Flach, Radiological Performance Assessment Date

TECHNICAL REVIEW:

T. S. Whiteside, Radiological Performance Assessment Date

APPROVAL:

D. A. Crowley, Manager Date
Radiological Performance Assessment

K. M. Kostelnik, Manager Date
Environmental Restoration Technologies

EXECUTIVE SUMMARY

Computational grids containing cell faces that do not align with an orthogonal (e.g. Cartesian, cylindrical) coordinate system are routinely encountered in porous-medium numerical simulations. Such grids are referred to in this study as *non-orthogonal* grids because some cell faces are not orthogonal to a coordinate system plane (e.g. *xy*, *yz* or *xz* plane in Cartesian coordinates). Non-orthogonal grids are routinely encountered at the Savannah River Site in porous-medium flow simulations for Performance Assessments and groundwater flow modeling. Examples include grid lines that conform to the sloping roof of a waste tank or disposal unit in a 2D Performance Assessment simulation, and grid surfaces that conform to undulating stratigraphic surfaces in a 3D groundwater flow model.

Particle tracking is routinely performed after a porous-medium numerical flow simulation to better understand the dynamics of the flow field and/or as an approximate indication of the trajectory and timing of advective solute transport. Particle tracks are computed by integrating the velocity field from cell to cell starting from designated seed (starting) positions. An accurate velocity field is required to attain accurate particle tracks. However, many numerical simulation codes report only the volumetric flowrate (e.g. PORFLOW) and/or flux (flowrate divided by area) crossing cell faces. For an *orthogonal* grid, the normal flux at a cell face is a component of the Darcy velocity vector in the coordinate system, and the pore velocity for particle tracking is attained by dividing by water content. For a *non-orthogonal* grid, the flux normal to a cell face that lies outside a coordinate plane is *not* a true component of velocity with respect to the coordinate system. Nonetheless, normal fluxes are often taken as Darcy velocity components, either naively or with accepted approximation.

To enable accurate particle tracking or otherwise present an accurate depiction of the velocity field for a non-orthogonal grid, Darcy velocity components are rigorously derived in this study from normal fluxes to cell faces, which are assumed to be provided by or readily computed from porous-medium simulation code output. The normal fluxes are presumed to satisfy mass balances for every computational cell, and if so, the derived velocity fields are consistent with these mass balances. Derivations are provided for general two-dimensional quadrilateral and three-dimensional hexagonal systems, and for the commonly encountered special cases of perfectly vertical side faces in 2D and 3D and a rectangular footprint in 3D.

TABLE OF CONTENTS

LIST OF TABLES

LIST OF FIGURES

LIST OF ABBREVIATIONS

2D	Two-Dimensional
3D	Three-Dimensional
FC	PORFLOW simulation code variable name for flowrates normal to cell faces
GSA	General Separations Area
QA	Quality Assurance
SRNL	Savannah River National Laboratory

1.0 Introduction

Computational grids containing cell faces that do not align with an orthogonal (e.g. Cartesian, cylindrical) coordinate system are routinely encountered in porous-medium numerical simulations. Such grids are referred to herein as *non-orthogonal* grids. Figure 1-1 illustrates two examples. The first example from Aleman (2007, Figure 4.4.3) is a two-dimensional grid composed of vertical grid lines parallel to the y-axis, but only nominally horizontal lines that are uniformly distributed to conform to a flat base and sloping ground surface. As a result all but the bottom grid line do not align with the *x*-axis. The second example from Flach (2004, Figure 2-1b) is a two-dimensional slice through the GSA/PORFLOW groundwater flow model. Here the nominally horizontal layers of the grid are not flat but conform to undulating stratigraphic surfaces. Again many cell faces do not align with the coordinate system (i.e. lie in constant *z* planes). In both grids depicted in Figure 1-1 the interior angles of a typical grid cell are not 90°. That attribute implies a non-orthogonal grid. However, a grid with all 90° angles between cell faces but rotated with respect to the coordinate system is also considered a non-orthogonal grid in this study, even though grid lines are orthogonal to one another. To be clear, an *orthogonal* grid contains only grid faces that are aligned to an orthogonal coordinate system (which implies 90° interior angles); if not, the grid is considered *non-orthogonal* (irrespective of the interior angles between cell faces, which could be 90°).

Particle tracking is routinely performed after a porous-medium numerical flow simulation to better understand the dynamics of the flow field and/or as an approximate indication of the trajectory and timing of advective solute transport. Particle tracks are computed by integrating the velocity field from cell to cell starting from designated seed (starting) positions. Obviously an accurate velocity field is required to attain accurate particle tracks. Many numerical simulation codes report only the volumetric flowrate and/or flux (flowrate divided by area) crossing cell faces. For an *orthogonal* grid, the normal flux at a cell face is a component of the Darcy velocity vector for the grid coordinate system, and the pore velocity is attained by dividing by water content. For a *non-orthogonal* grid, the flux normal to a cell face that lies outside a coordinate plane (e.g. constant *x*, *y*, or *z* plane in a Cartesian system) is *not* a true component of the velocity vector. Nonetheless, normal fluxes are often used as Darcy velocity components, either naively or with accepted approximation.

The purpose of this study is to derive the true Darcy velocity components from normal fluxes to cell faces on a non-orthogonal grid to enable accurate particle tracking. The normal fluxes are presumed to satisfy mass balances for every computational cell. Derivations are provided for general two-dimensional quadrilateral and three-dimensional hexagonal systems, and for the commonly encountered special cases of perfectly vertical side faces in 2D and 3D. The derived velocity fields are consistent with the normal fluxes and thus preserve mass.

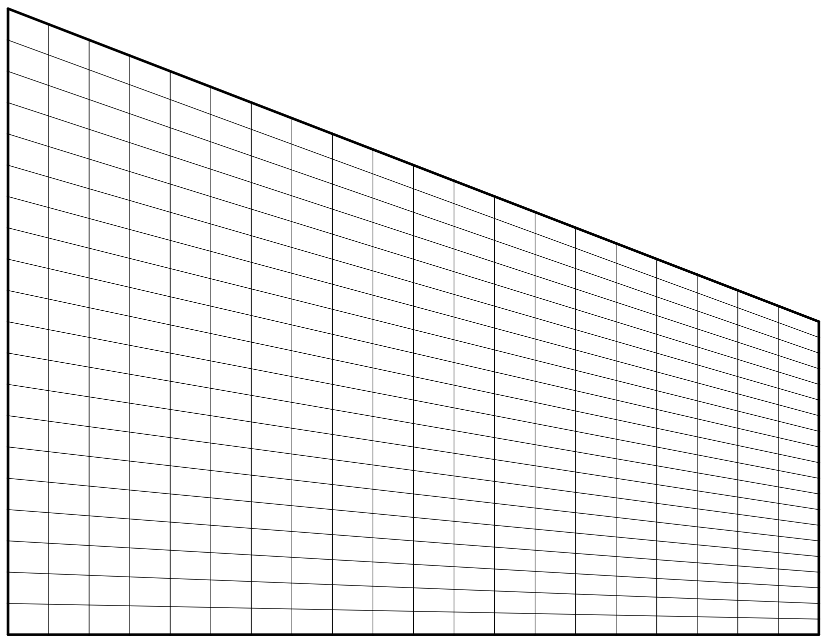

(a)

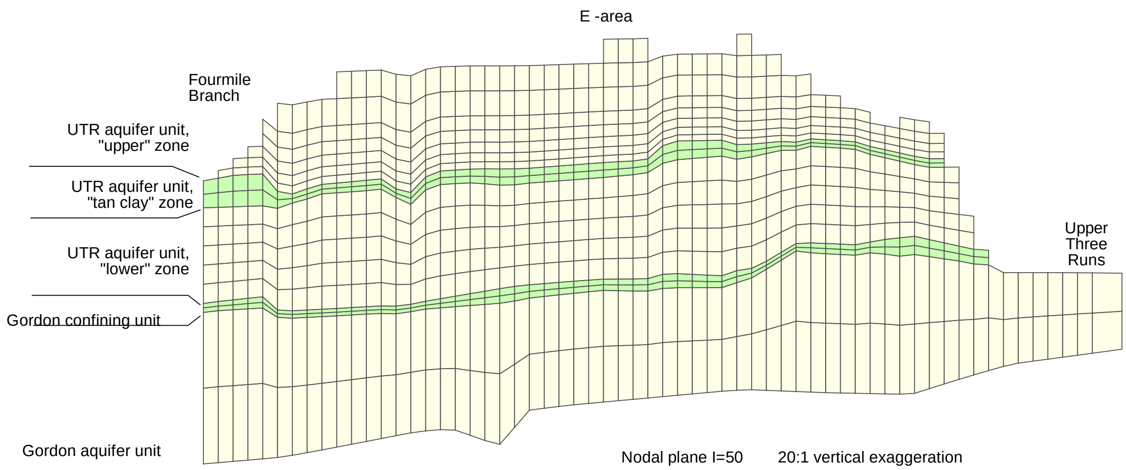

(b)

Figure 1-1. Example non-orthogonal numerical grids: a) PORFLOW QA test problem 4.4 (WSRC-STI-2007-00150 Figure 4.4.3) and b) grid cross-section from GSA/PORFLOW groundwater flow model (WSRC-TR-2004-00106 Figure 2-1).

2.0 Two-Dimensional Grid

Figure 2-1 depicts a representative non-orthogonal quadrilateral grid cell. In this two-dimensional example all four cell faces lie at an angle to the orthogonal coordinate system defined by the unit vectors $\vec{\imath}$, $\vec{\jmath}$ and $\vec{k}$ (where $\vec{k}$ points out of the page). The four vertices are denoted by *mm*, *mp*, *pm* and *pp* (*m* = minus, *p* = plus position relative to cell center). The velocity vector at the center of the cell is denoted by $\vec{v}$. A local grid coordinate system, generally non-orthogonal, is indicated by the vectors $\vec{X}$ and $\vec{Y}$. By definition $\vec{X}$ bisects the *mm*-*mp* and *pm*-*pp* faces. Similarly $\vec{Y}$ bisects the *mm*-*pm* and *mp*-*pp* faces.

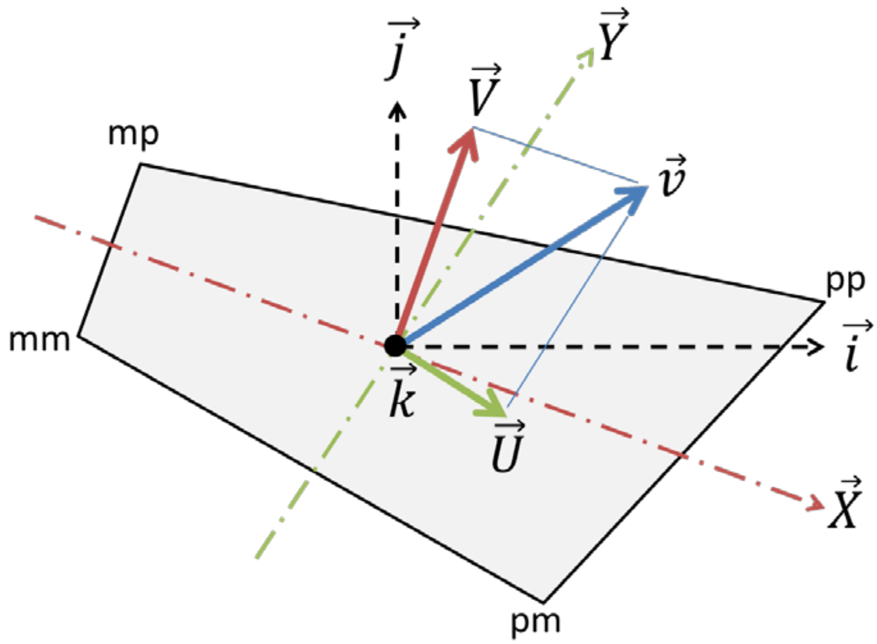

Figure 2-1. Coordinate systems, velocity field, and normal flux components for a non-orthogonal computational grid cell.

The local grid coordinate vectors are thus computed as

$$\vec{X} = \left(\frac{x_{pm} + x_{pp}}{2} - \frac{x_{mm} + x_{mp}}{2}\right)\vec{\imath} + \left(\frac{y_{pm} + y_{pp}}{2} - \frac{y_{mm} + y_{mp}}{2}\right)\vec{\jmath} \quad (1)$$

and

$$\vec{Y} = \left(\frac{x_{mp} + x_{pp}}{2} - \frac{x_{mm} + x_{pm}}{2}\right)\vec{\imath} + \left(\frac{y_{mp} + y_{pp}}{2} - \frac{y_{mm} + y_{pm}}{2}\right)\vec{\jmath} \quad (2)$$

The unit vectors for the local grid coordinate system are

$$\vec{x} = \frac{\vec{X}}{|\vec{X}|} \quad (3)$$

and

$$\vec{y} = \frac{\vec{Y}}{|\vec{Y}|} \tag{4}$$

Also shown in Figure 2-1 are the components of velocity $\vec{v}$ normal to $\vec{X}$ (and $\vec{x}$) and $\vec{Y}$ (and $\vec{y}$) denoted as $\vec{V}$ and $\vec{U}$ respectively. Note that although $\vec{U}$ is nominally in the direction of $\vec{X}$, the two vectors are not generally parallel, and similarly for $\vec{V}$ and $\vec{Y}$. Rather $\vec{U}$ is perpendicular to $\vec{Y}$ and $\vec{V}$ is perpendicular to $\vec{X}$.

The magnitude of $\vec{U}$ is assumed to be available from the computational code output and abbreviated as U. The flux U may be directly provided in simulation code output, or more likely, defined as the average of the normal fluxes provided at the *mm-mp* and *pm-pp* faces.

$$|\vec{U}| \equiv U = \frac{U_{mm-mp} + U_{pm-pp}}{2} \tag{5}$$

The PORFLOW code for example provides flow rates crossing cell faces, and flux can be attained by dividing by face length (or area in 3D). Similarly, $\vec{V}$ is considered a known quantity defined by

$$|\vec{V}| \equiv V = \frac{V_{mm-pm} + V_{mp-pp}}{2} \tag{6}$$

The normal fluxes can be related to the velocity field using vector operations. A vector normal to $\vec{y}$ is the cross product $\vec{y} \times \vec{k}$ (see Swokowski (1979) Figure 14.30 or http://en.wikipedia.org/wiki/Cross_product):

$$\vec{y} \times \vec{k} = \begin{vmatrix} \vec{\imath} & \vec{\jmath} & \vec{k} \\ y_1 & y_2 & 0 \\ 0 & 0 & 1 \end{vmatrix} = y_2\vec{\imath} - y_1\vec{\jmath} \tag{7}$$

The vector $\vec{y} \times \vec{k}$ has unit length:

$$|\vec{y} \times \vec{k}| = \sqrt{y_2^2 + y_1^2} = |\vec{y}| = 1 \tag{8}$$

The component of $\vec{v}$ parallel to $\vec{y} \times \vec{k}$ and thus normal to $\vec{y}$ is obtained by forming the vector dot product (see Swokowski (1979), Equation (14.24) or http://en.wikipedia.org/wiki/Dot_product)

$$U = \vec{v} \cdot \frac{\vec{y} \times \vec{k}}{|\vec{y} \times \vec{k}|} = (v_1\vec{\imath} + v_2\vec{\jmath}) \cdot (y_2\vec{\imath} - y_1\vec{\jmath}) = v_1 y_2 - v_2 y_1 \tag{9}$$

In a similar manner, $\vec{k} \times \vec{x}$ (recalling the right-hand rule for vector products) is a unit normal vector to $\vec{x}$

$$\vec{k} \times \vec{x} = \begin{vmatrix} \vec{\imath} & \vec{\jmath} & \vec{k} \\ 0 & 0 & 1 \\ x_1 & x_2 & 0 \end{vmatrix} = -x_2\vec{\imath} + x_1\vec{\jmath} \tag{10}$$

and the component of $\vec{v}$ normal to $\vec{x}$ is

$$V = \vec{v} \cdot \frac{\vec{k} \times \vec{x}}{|\vec{k} \times \vec{x}|} = (v_1 \vec{\imath} + v_2 \vec{\jmath}) \cdot (-x_2 \vec{\imath} + x_1 \vec{\jmath}) = -v_1 x_2 + v_2 x_1 \tag{11}$$

Equations (9) and (11) can be solved simultaneously for v_1 and v_2 using Cramer's rule (http://en.wikipedia.org/wiki/Cramer%27s_rule). The results are

$$v_1 = \frac{\begin{vmatrix} U & -y_1 \\ V & x_1 \end{vmatrix}}{\begin{vmatrix} y_2 & -y_1 \\ -x_2 & x_1 \end{vmatrix}} = \frac{Ux_1 - (-y_1)V}{y_2 x_1 - (-y_1)(-x_2)} = \frac{x_1 U + y_1 V}{x_1 y_2 - x_2 y_1} \tag{12}$$

and

$$v_2 = \frac{\begin{vmatrix} y_2 & U \\ -x_2 & V \end{vmatrix}}{\begin{vmatrix} y_2 & -y_1 \\ -x_2 & x_1 \end{vmatrix}} = \frac{y_2 V - U(-x_2)}{y_2 x_1 - (-y_1)(-x_2)} = \frac{x_2 U + y_2 V}{x_1 y_2 - x_2 y_1} \tag{13}$$

Equations (12) and (13) define velocity $\vec{v}$ in terms of the known geometry of the grid cell $(\vec{x}, \vec{y})$ and known normal flux components (U, V) for a general two-dimensional system.

A special case of interest is a grid with perfectly vertical sides, such as the example shown in Figure 1-1a. For this case

$$\vec{y} = \vec{\jmath} = 0 \cdot \vec{\imath} + 1 \cdot \vec{\jmath} \tag{14}$$

and thus $y_1 = 0$ and $y_2 = 1$. Equations (12) and (13) simplify to

$$v_1 = U \tag{15}$$

and

$$v_2 = \frac{1}{x_1} V + \frac{x_2}{x_1} U \tag{16}$$

Equations (12), (13), (15) and (16) account for a distorted and/or rotated mesh through the geometric factors x_1, x_2, y_1 and y_2 and make appropriate perturbations to the nominal velocity components U and V.

Figure 2-2 compares particle tracking results based Darcy velocity approximated by $U\vec{\imath} + V\vec{\jmath}$ and rigorously defined by $v_1 \vec{\imath} + v_2 \vec{\jmath}$. The problem specification is the same as PORFLOW QA test problem 4.4 (Aleman 2007), except that the recharge is set to zero (no infiltration). Using $\vec{v} \equiv U\vec{\imath} + V\vec{\jmath}$ particle tracks are observed to angle upward and cross the water table because grid distortion has not been considered. However, when Darcy velocity is defined by $\vec{v} \equiv v_1 \vec{\imath} + v_2 \vec{\jmath}$ the streamtraces conform to the water table as expected.

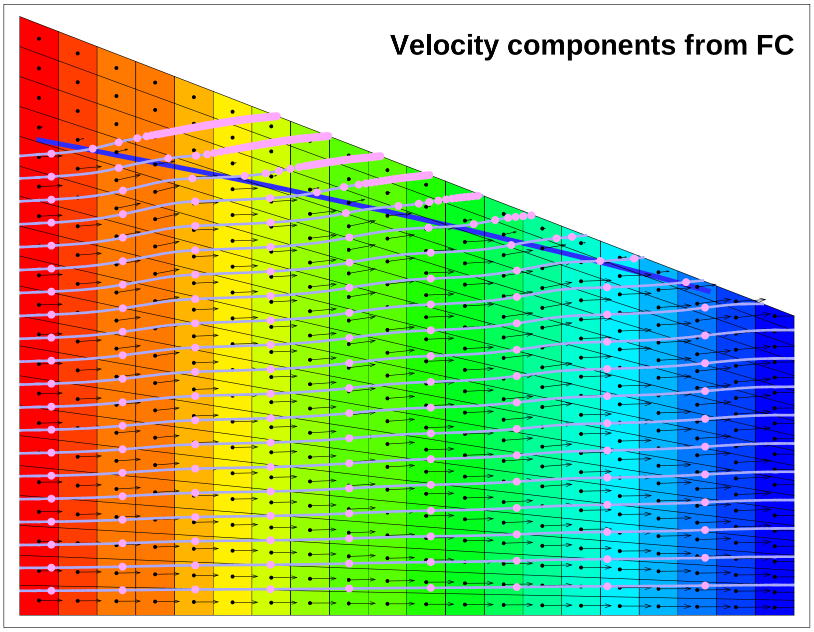

(a)

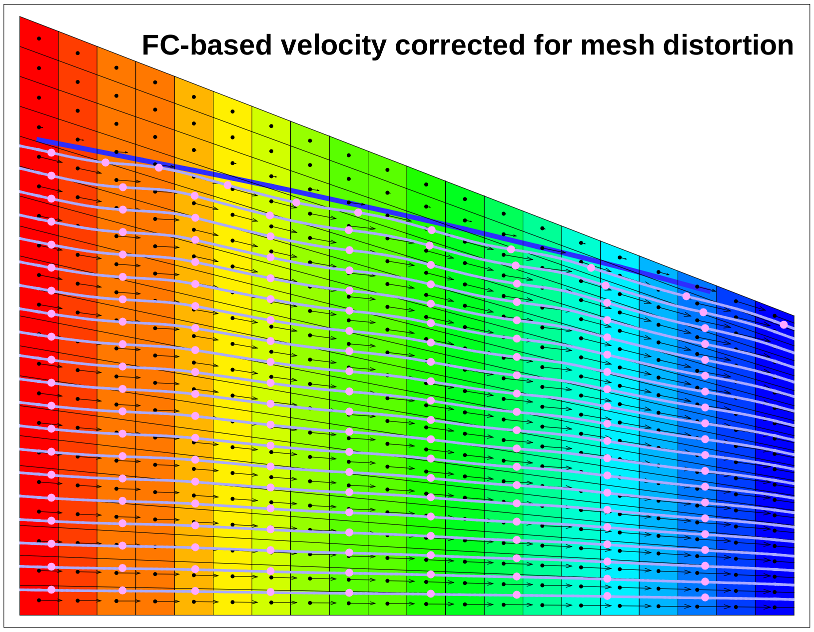

(b)

Figure 2-2. Particle tracking based on Darcy velocity (a) approximated by $U\vec{\imath} + V\vec{\jmath}$ and (b) rigorously defined as $v_1\vec{\imath} + v_2\vec{\jmath}$ – Cartesian coordinates.

Figure 2-3 illustrates particle tracking results for a cylindrical coordinate system simulation similar to PORFLOW QA test problem 4.4 (Aleman 2007). As with prior Cartesian simulation, the recharge rate is set to zero. In addition the $\vec{\imath}$ coordinates are reinterpreted as radial distance and the inner and outer radii are set to 100 ft and 1100 ft respectively. The hollow cylinder geometry produces a concave upward water table. Particle tracks behave similar to those shown in Figure 2-2. When Darcy velocity is defined by $\vec{v} \equiv v_1\vec{\imath} + v_2\vec{\jmath}$ the streamtraces conform to the water table as expected.

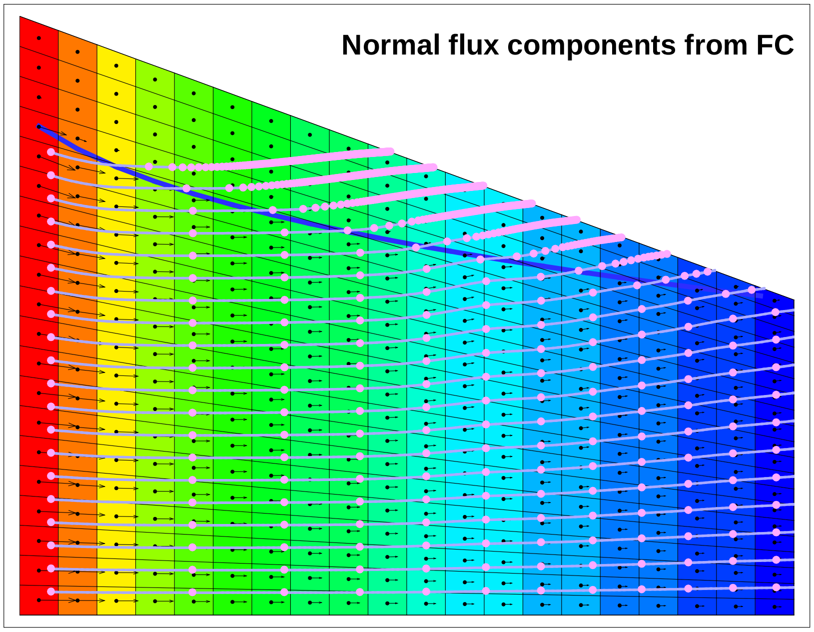

(a)

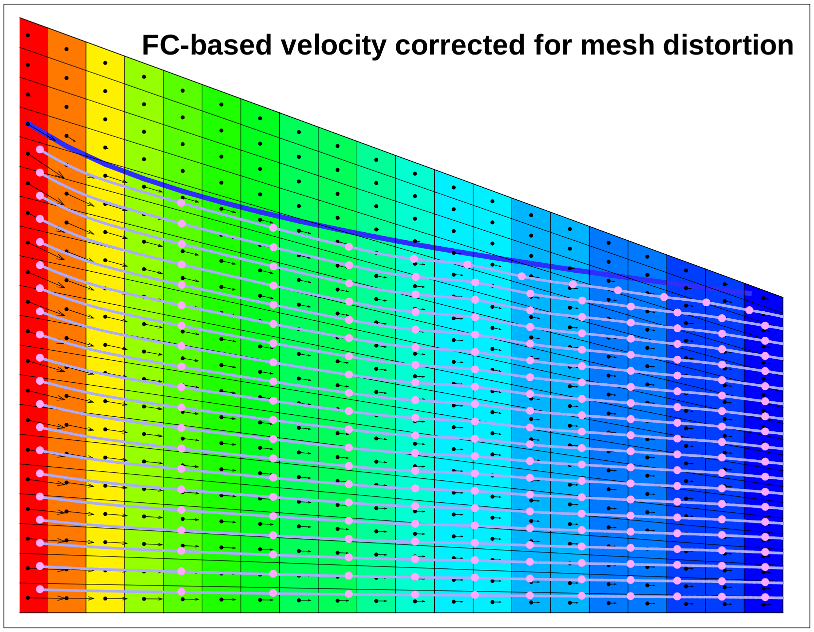

(b)

Figure 2-3. Particle tracking based on Darcy velocity (a) approximated by $U\vec{\imath} + V\vec{\jmath}$ and (b) rigorously defined as $v_1\vec{\imath} + v_2\vec{\jmath}$ – cylindrical coordinates.

3.0 Three-Dimensional Grid

Figure 3-1 illustrates a three-dimensional hexagonal grid cell that generally has faces not aligned with an $\vec{\imath} \times \vec{\jmath}$, $\vec{\jmath} \times \vec{k}$ or $\vec{k} \times \vec{\imath}$ coordinate plane. The eight vertices are identified using *m* and *p* indices analogous to the 2D grid cell shown in Figure 2-1. For example, *mpm* identifies the corner located minus, plus, minus relative to the center node in the $\vec{\imath}$, $\vec{\jmath}$ and $\vec{k}$ coordinate directions, respectively. A local grid coordinate system is indicated by the vectors $\vec{X}$, $\vec{Y}$ and $\vec{Z}$, which are generally not orthogonal. These vectors pass through the centroids of opposing cell faces and are defined by the equations

$$\vec{X} = \left(\frac{x_{pmm} + x_{ppm} + x_{pmp} + x_{ppp}}{4} - \frac{x_{mmm} + x_{mpm} + x_{mmp} + x_{mpp}}{4}\right)\vec{\imath} + \cdots \quad (17)$$

$$\vec{Y} = \left(\frac{x_{mpm} + x_{ppm} + x_{mpp} + x_{ppp}}{4} - \frac{x_{mmm} + x_{pmm} + x_{mmp} + x_{pmp}}{4}\right)\vec{\imath} + \cdots \quad (18)$$

and

$$\vec{Z} = \left(\frac{x_{mmp} + x_{pmp} + x_{mpp} + x_{ppp}}{4} - \frac{x_{mmm} + x_{pmm} + x_{mpm} + x_{ppm}}{4}\right)\vec{\imath} + \cdots \quad (19)$$

Defined in this way the vectors intersect one another at the centroid of the volume. The corresponding unit vectors are denoted by $\vec{x}$, $\vec{y}$ and $\vec{z}$. Volumetric flux normal to each cell face is assumed to available from simulation code output.

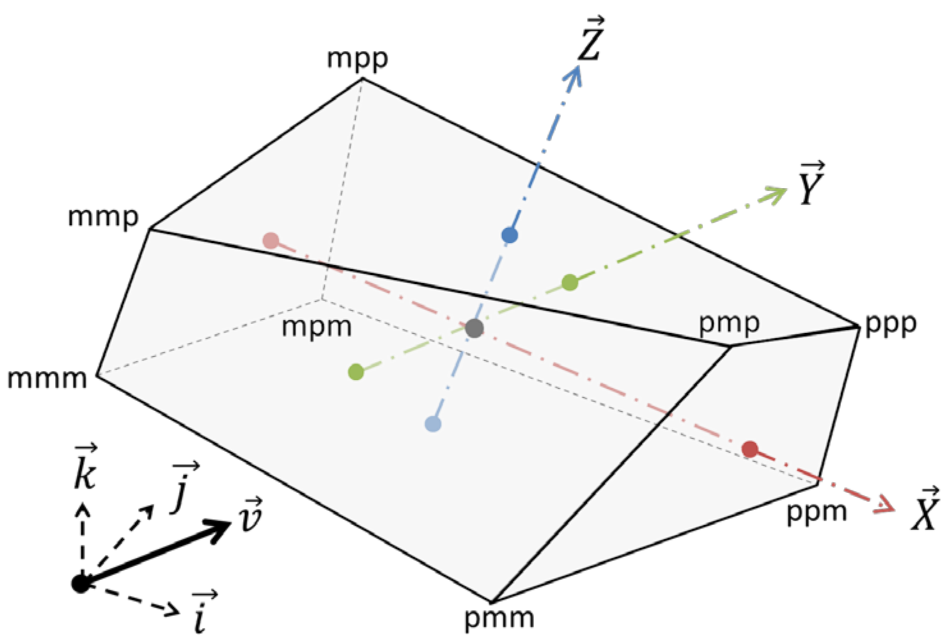

Figure 3-1. Coordinate systems and velocity vector for a non-orthogonal three-dimensional grid cell.

The flux in the nominal direction of $\vec{X}$ at the cell centroid is defined as the average of the fluxes at the $\vec{X}^-$ and $\vec{X}^+$ faces

$$|\vec{U}| \equiv U = \frac{U_{mmm-mpm-mmp-mpp} + U_{pmm-ppm-pmp-ppp}}{2} \tag{20}$$

V and W fluxes are defined for the other coordinates in a similar manner.

The flux U is normal to the plane

$$\vec{y} \times \vec{z} = \begin{vmatrix} \vec{\imath} & \vec{\jmath} & \vec{k} \\ y_1 & y_2 & y_3 \\ z_1 & z_2 & z_3 \end{vmatrix} = (y_2 z_3 - y_3 z_2)\vec{\imath} - (y_1 z_3 - y_3 z_1)\vec{\jmath} + (y_1 z_2 - y_2 z_1)\vec{k} \tag{21}$$

and defined in terms of $\vec{v}$ by

$$\begin{aligned} U &= \vec{v} \cdot \frac{\vec{y} \times \vec{z}}{|\vec{y} \times \vec{z}|} \\ &= \frac{\left(v_1\vec{\imath} + v_2\vec{\jmath} + v_3\vec{k}\right) \cdot \left[(y_2 z_3 - y_3 z_2)\vec{\imath} - (y_1 z_3 - y_3 z_1)\vec{\jmath} + (y_1 z_2 - y_2 z_1)\vec{k}\right]}{|\vec{y} \times \vec{z}|} \\ &= \frac{v_1(y_2 z_3 - y_3 z_2) - v_2(y_1 z_3 - y_3 z_1) + v_3(y_1 z_2 - y_2 z_1)}{|\vec{y} \times \vec{z}|} \\ &= \frac{v_1(y_2 z_3 - y_3 z_2) + v_2(y_3 z_1 - y_1 z_3) + v_3(y_1 z_2 - y_2 z_1)}{|\vec{y} \times \vec{z}|} \\ &= \frac{y_2 z_3 - y_3 z_2}{|\vec{y} \times \vec{z}|} v_1 + \frac{y_3 z_1 - y_1 z_3}{|\vec{y} \times \vec{z}|} v_2 + \frac{y_1 z_2 - y_2 z_1}{|\vec{y} \times \vec{z}|} v_3 \equiv a_{yz} v_1 + b_{yz} v_2 + c_{yz} v_3 \end{aligned} \tag{22}$$

The flux V is normal to the plane

$$\vec{z} \times \vec{x} = \begin{vmatrix} \vec{\imath} & \vec{\jmath} & \vec{k} \\ z_1 & z_2 & z_3 \\ x_1 & x_2 & x_3 \end{vmatrix} = (x_3 z_2 - x_2 z_3)\vec{\imath} - (x_3 z_1 - x_1 z_3)\vec{\jmath} + (x_2 z_1 - x_1 z_2)\vec{k} \tag{23}$$

and defined in terms of $\vec{v}$ by

$$\begin{aligned} V &= \vec{v} \cdot \frac{\vec{z} \times \vec{x}}{|\vec{z} \times \vec{x}|} \\ &= \frac{\left(v_1\vec{\imath} + v_2\vec{\jmath} + v_3\vec{k}\right) \cdot \left[(x_3 z_2 - x_2 z_3)\vec{\imath} - (x_3 z_1 - x_1 z_3)\vec{\jmath} + (x_2 z_1 - x_1 z_2)\vec{k}\right]}{|\vec{z} \times \vec{x}|} \\ &= \frac{v_1(x_3 z_2 - x_2 z_3) - v_2(x_3 z_1 - x_1 z_3) + v_3(x_2 z_1 - x_1 z_2)}{|\vec{z} \times \vec{x}|} \\ &= \frac{v_1(x_3 z_2 - x_2 z_3) + v_2(x_1 z_3 - x_3 z_1) + v_3(x_2 z_1 - x_1 z_2)}{|\vec{z} \times \vec{x}|} \\ &= \frac{x_3 z_2 - x_2 z_3}{|\vec{z} \times \vec{x}|} v_1 + \frac{x_1 z_3 - x_3 z_1}{|\vec{z} \times \vec{x}|} v_2 + \frac{x_2 z_1 - x_1 z_2}{|\vec{z} \times \vec{x}|} v_3 \equiv a_{xz} v_1 + b_{xz} v_2 + c_{xz} v_3 \end{aligned} \tag{24}$$

The flux W is normal to the plane

$$\vec{x} \times \vec{y} = \begin{vmatrix} \vec{\imath} & \vec{\jmath} & \vec{k} \\ x_1 & x_2 & x_3 \\ y_1 & y_2 & y_3 \end{vmatrix} = (x_2 y_3 - x_3 y_2)\vec{\imath} - (x_1 y_3 - x_3 y_1)\vec{\jmath} + (x_1 y_2 - x_2 y_1)\vec{k} \quad (25)$$

and defined in terms of $\vec{v}$ by

$$\begin{aligned} W &= \vec{v} \cdot \frac{\vec{x} \times \vec{y}}{|\vec{x} \times \vec{y}|} \\ &= \frac{\left(v_1\vec{\imath} + v_2\vec{\jmath} + v_3\vec{k}\right) \cdot \left[(x_2 y_3 - x_3 y_2)\vec{\imath} - (x_1 y_3 - x_3 y_1)\vec{\jmath} + (x_1 y_2 - x_2 y_1)\vec{k}\right]}{|\vec{x} \times \vec{y}|} \\ &= \frac{v_1(x_2 y_3 - x_3 y_2) - v_2(x_1 y_3 - x_3 y_1) + v_3(x_1 y_2 - x_2 y_1)}{|\vec{x} \times \vec{y}|} \\ &= \frac{v_1(x_2 y_3 - x_3 y_2) + v_2(x_3 y_1 - x_1 y_3) + v_3(x_1 y_2 - x_2 y_1)}{|\vec{x} \times \vec{y}|} \\ &= \frac{x_2 y_3 - x_3 y_2}{|\vec{x} \times \vec{y}|} v_1 + \frac{x_3 y_1 - x_1 y_3}{|\vec{x} \times \vec{y}|} v_2 + \frac{x_1 y_2 - x_2 y_1}{|\vec{x} \times \vec{y}|} v_3 \\ &\equiv a_{xy} v_1 + b_{xy} v_2 + c_{xy} v_3 \end{aligned} \quad (26)$$

Equations (22), (24) and (26) represent a system of three equations for three unknowns, v_1, v_2 and v_3, summarized by

$$\begin{cases} a_{yz} v_1 + b_{yz} v_2 + c_{yz} v_3 = U \\ a_{xz} v_1 + b_{xz} v_2 + c_{xz} v_3 = V \\ a_{xy} v_1 + b_{xy} v_2 + c_{xy} v_3 = W \end{cases} \quad (27)$$

The system can be solved using Cramer's rule (http://en.wikipedia.org/wiki/Cramer%27s_rule). The results are

$$\begin{aligned} v_1 &= \begin{vmatrix} U & b_{yz} & c_{yz} \\ V & b_{xz} & c_{xz} \\ W & b_{xy} & c_{xy} \end{vmatrix} \Big/ \begin{vmatrix} a_{yz} & b_{yz} & c_{yz} \\ a_{xz} & b_{xz} & c_{xz} \\ a_{xy} & b_{xy} & c_{xy} \end{vmatrix} \\ &= \frac{U\left(b_{xz} c_{xy} - b_{xy} c_{xz}\right) - V\left(b_{yz} c_{xy} - b_{xy} c_{yz}\right) + W\left(b_{yz} c_{xz} - b_{xz} c_{yz}\right)}{\begin{vmatrix} a_{yz} & b_{yz} & c_{yz} \\ a_{xz} & b_{xz} & c_{xz} \\ a_{xy} & b_{xy} & c_{xy} \end{vmatrix}} \end{aligned} \quad (28)$$

$$\begin{aligned} v_2 &= \begin{vmatrix} a_{yz} & U & c_{yz} \\ a_{xz} & V & c_{xz} \\ a_{xy} & W & c_{xy} \end{vmatrix} \Big/ \begin{vmatrix} a_{yz} & b_{yz} & c_{yz} \\ a_{xz} & b_{xz} & c_{xz} \\ a_{xy} & b_{xy} & c_{xy} \end{vmatrix} \\ &= \frac{-U\left(a_{xz} c_{xy} - a_{xy} c_{xz}\right) + V\left(a_{yz} c_{xy} - a_{xy} c_{yz}\right) - W\left(a_{yz} c_{xz} - a_{xz} c_{yz}\right)}{\begin{vmatrix} a_{yz} & b_{yz} & c_{yz} \\ a_{xz} & b_{xz} & c_{xz} \\ a_{xy} & b_{xy} & c_{xy} \end{vmatrix}} \end{aligned} \quad (29)$$

and

$$v_3 = \begin{vmatrix} a_{yz} & b_{yz} & U \\ a_{xz} & b_{xz} & V \\ a_{xy} & b_{xy} & W \end{vmatrix} \Bigg/ \begin{vmatrix} a_{yz} & b_{yz} & c_{yz} \\ a_{xz} & b_{xz} & c_{xz} \\ a_{xy} & b_{xy} & c_{xy} \end{vmatrix}$$
$$= \frac{U\left(a_{xz}b_{xy} - a_{xy}b_{xz}\right) - V\left(a_{yz}b_{xy} - a_{xy}b_{yz}\right) + W\left(a_{yz}b_{xz} - a_{xz}b_{yz}\right)}{\begin{vmatrix} a_{yz} & b_{yz} & c_{yz} \\ a_{xz} & b_{xz} & c_{xz} \\ a_{xy} & b_{xy} & c_{xy} \end{vmatrix}} \tag{30}$$

where

$$\begin{vmatrix} a_{yz} & b_{yz} & c_{yz} \\ a_{xz} & b_{xz} & c_{xz} \\ a_{xy} & b_{xy} & c_{xy} \end{vmatrix}$$
$$\begin{aligned} &= a_{yz}\left(b_{xz}c_{xy} - b_{xy}c_{xz}\right) + a_{xz}\left(b_{xy}c_{yz} - b_{yz}c_{xy}\right) \\ &+ a_{xy}\left(b_{yz}c_{xz} - b_{xz}c_{yz}\right) \\ &= a_{yz}b_{xz}c_{xy} - a_{yz}b_{xy}c_{xz} + a_{xz}b_{xy}c_{yz} - a_{xz}b_{yz}c_{xy} \\ &+ a_{xy}b_{yz}c_{xz} - a_{xy}b_{xz}c_{yz} \end{aligned} \tag{31}$$

A common special case is a 3D grid with vertical sides and rectangular footprint. The GSA/PORFLOW groundwater flow model (Flach 2004) is an example of such a "cookie cutter" grid. For this special case the following simplifications occur

$$\vec{z} = \vec{k} \quad \rightarrow \quad z_1 = z_2 = 0; z_3 = 1 \tag{32}$$

$$x_2 = y_1 = 0 \tag{33}$$

The a, b and c coefficients evaluate to

$$\begin{array}{ccc} a_{yz} = 1 & b_{yz} = 0 & c_{yz} = 0 \\ a_{xz} = 0 & b_{xz} = 1 & c_{xz} = 0 \\ a_{xy} = \dfrac{-x_3 y_2}{|\vec{x} \times \vec{y}|} & b_{xy} = \dfrac{-x_1 y_3}{|\vec{x} \times \vec{y}|} & c_{xy} = \dfrac{x_1 y_2}{|\vec{x} \times \vec{y}|} \end{array} \tag{34}$$

where

$$|\vec{x} \times \vec{y}| = \sqrt{(x_3 y_2)^2 + (x_1 y_3)^2 + (x_1 y_2)^2} \tag{35}$$

The determinant given by Equation (31) becomes

$$\begin{vmatrix} a_{yz} & b_{yz} & c_{yz} \\ a_{xz} & b_{xz} & c_{xz} \\ a_{xy} & b_{xy} & c_{xy} \end{vmatrix} = c_{xy} = \frac{(x_1 y_2)^2}{|\vec{x} \times \vec{y}|} \tag{36}$$

Using Equations (28) and (29) , the horizontal velocity components simplify to

$$v_1 = \frac{U(c_{xy})}{c_{xy}} = U \tag{37}$$

and

$$v_2 = \frac{V(c_{xy})}{c_{xy}} = V \tag{38}$$

The vertical component from Equation (30) is

$$\begin{aligned} v_3 &= \frac{U(-a_{xy}) - V(b_{xy}) + W(1)}{c_{xy}} = \frac{U\left(\frac{x_3 y_2}{|\vec{x} \times \vec{y}|}\right) + V\left(\frac{x_1 y_3}{|\vec{x} \times \vec{y}|}\right) + W(1)}{\frac{x_1 y_2}{|\vec{x} \times \vec{y}|}} \\ &= \frac{U x_3 y_2 + V x_1 y_3 + W|\vec{x} \times \vec{y}|}{x_1 y_2} = \frac{x_3}{x_1} U + \frac{y_3}{y_2} V + \frac{|\vec{x} \times \vec{y}|}{x_1 y_2} W \\ &= \frac{x_3}{x_1} U + \frac{y_3}{y_2} V + \frac{\sqrt{(x_3 y_2)^2 + (x_1 y_3)^2 + (x_1 y_2)^2}}{x_1 y_2} W \\ &= \sqrt{1 + \left(\frac{x_3}{x_1}\right)^2 + \left(\frac{y_3}{y_2}\right)^2}\, W + \frac{x_3}{x_1} U + \frac{y_3}{y_2} V \end{aligned} \tag{39}$$

These results for the three-dimensional special case are similar to those for the two-dimensional special case given by Equations (15) and (16). Namely, each horizontal velocity component is equal to its corresponding horizontal normal flux, while the vertical velocity component is a function of all of the normal fluxes.

4.0 Conclusions

The derivations presented herein provide a means to perform accurate particle-tracking on non-orthogonal grids, or otherwise present an accurate depiction of the velocity field, based on normal fluxes to cell faces provided by or readily computed from porous-medium simulation code output. The velocity vector components for a general grid are given by Equations (12) and (13) for 2D systems and Equations (28) through (31) for 3D systems. Simplified results are presented for 2D and 3D grids that have strictly vertical side faces and a rectangular footprint if 3D, conditions routinely encountered in Savannah River Performance Assessment applications and groundwater flow modeling. These are Equations (15) and (16) in 2D and (37), (38) and (39) in 3D. These key results are summarized in Table 4-1.

Table 4-1. Summary of velocity vector components in terms of normal fluxes.

General 2D grid

$$v_1 = \frac{x_1 U + y_1 V}{x_1 y_2 - x_2 y_1} \qquad v_2 = \frac{x_2 U + y_2 V}{x_1 y_2 - x_2 y_1}$$

2D grid with vertical side faces

$$v_1 = U \qquad v_2 = \frac{1}{x_1} V + \frac{x_2}{x_1} U$$

General 3D grid

$$v_1 = \left[U\left(b_{xz}c_{xy} - b_{xy}c_{xz}\right) - V\left(b_{yz}c_{xy} - b_{xy}c_{yz}\right) + W\left(b_{yz}c_{xz} - b_{xz}c_{yz}\right)\right] \Big/ \begin{vmatrix} a_{yz} & b_{yz} & c_{yz} \\ a_{xz} & b_{xz} & c_{xz} \\ a_{xy} & b_{xy} & c_{xy} \end{vmatrix}$$

$$v_2 = \left[-U\left(a_{xz}c_{xy} - a_{xy}c_{xz}\right) + V\left(a_{yz}c_{xy} - a_{xy}c_{yz}\right) - W\left(a_{yz}c_{xz} - a_{xz}c_{yz}\right)\right] \Big/ \begin{vmatrix} a_{yz} & b_{yz} & c_{yz} \\ a_{xz} & b_{xz} & c_{xz} \\ a_{xy} & b_{xy} & c_{xy} \end{vmatrix}$$

$$v_3 = \left[U\left(a_{xz}b_{xy} - a_{xy}b_{xz}\right) - V\left(a_{yz}b_{xy} - a_{xy}b_{yz}\right) + W\left(a_{yz}b_{xz} - a_{xz}b_{yz}\right)\right] \Big/ \begin{vmatrix} a_{yz} & b_{yz} & c_{yz} \\ a_{xz} & b_{xz} & c_{xz} \\ a_{xy} & b_{xy} & c_{xy} \end{vmatrix}$$

$$\begin{vmatrix} a_{yz} & b_{yz} & c_{yz} \\ a_{xz} & b_{xz} & c_{xz} \\ a_{xy} & b_{xy} & c_{xy} \end{vmatrix} = a_{yz}b_{xz}c_{xy} - a_{yz}b_{xy}c_{xz} + a_{xz}b_{xy}c_{yz} - a_{xz}b_{yz}c_{xy} + a_{xy}b_{yz}c_{xz} - a_{xy}b_{xz}c_{yz}$$

$$a_{yz} = \frac{y_2 z_3 - y_3 z_2}{|\vec{y} \times \vec{z}|} \quad b_{yz} = \frac{y_3 z_1 - y_1 z_3}{|\vec{y} \times \vec{z}|} \quad c_{yz} = \frac{y_1 z_2 - y_2 z_1}{|\vec{y} \times \vec{z}|}$$

$$a_{xz} = \frac{x_3 z_2 - x_2 z_3}{|\vec{z} \times \vec{x}|} \quad b_{xz} = \frac{x_1 z_3 - x_3 z_1}{|\vec{z} \times \vec{x}|} \quad c_{xz} = \frac{x_2 z_1 - x_1 z_2}{|\vec{z} \times \vec{x}|}$$

$$a_{xy} = \frac{x_2 y_3 - x_3 y_2}{|\vec{x} \times \vec{y}|} \quad b_{xy} = \frac{x_3 y_1 - x_1 y_3}{|\vec{x} \times \vec{y}|} \quad c_{xy} = \frac{x_1 y_2 - x_2 y_1}{|\vec{x} \times \vec{y}|}$$

$$|\vec{y} \times \vec{z}| = \sqrt{(y_2 z_3 - y_3 z_2)^2 + (y_1 z_3 - y_3 z_1)^2 + (y_1 z_2 - y_2 z_1)^2}$$

$$|\vec{z} \times \vec{x}| = \sqrt{(x_3 z_2 - x_2 z_3)^2 + (x_3 z_1 - x_1 z_3)^2 + (x_2 z_1 - x_1 z_2)^2}$$

$$|\vec{x} \times \vec{y}| = \sqrt{(x_2 y_3 - x_3 y_2)^2 + (x_1 y_3 - x_3 y_1)^2 + (x_1 y_2 - x_2 y_1)^2}$$

3D grid with vertical side faces and rectangular footprint

$$v_1 = U \qquad v_2 = V$$

$$v_3 = \sqrt{1 + \left(\frac{x_3}{x_1}\right)^2 + \left(\frac{y_3}{y_2}\right)^2}\, W + \frac{x_3}{x_1} U + \frac{y_3}{y_2} V$$

5.0 References

Aleman, S. E. *PORFLOW Testing and Verification Document*. WSRC-STI-2007-00150, Rev 0. June 2007.

Flach, G. P. *Groundwater Flow Model of the General Separations Area Using Porflow (U)*. WSRC-TR-2004-00106, Rev. 0. July 2004.

Swokowski, E. W. *Calculus with Analytic Geometry; Second Edition*. Prindle, Weber & Schmidt, Boston MA. 999 pages. 1979.

Distribution:

B. T. Butcher, 773-43A
G. P. Flach, 773-42A
R. A. Hiergesell, 773-43A
M. A. Phifer, 773-42A
R. R. Seitz, 773-43A
F. G. Smith, III 703-41A
G. A. Taylor, 773-43A
T. Whiteside, 773-42A
S. E. Aleman, 735-A
L. L. Hamm, 735-A
G. K. Humphries, 730-4B
D. A. Crowley, 773-43A
T. O. Oliver, 773-42A
J. J. Mayer, 773-42A
K. M. Kostelnik, 773-42A
J. C. Griffin, 773-A
S. L. Marra, 773-A
Records Administration (EDWS)